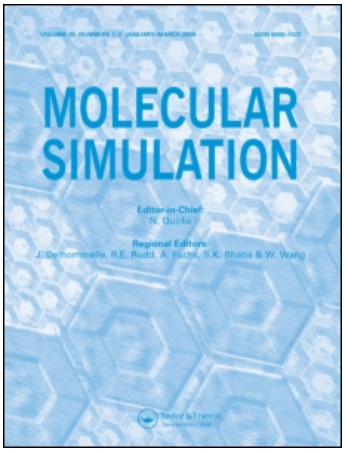

Molecular Simulation
Publication details, including instructions for authors and subscription information:
http://www.informaworld.com/smpp/title~content=t713644482

Molecular Dynamics Simulation of Hexamine and Suberic Acid

Yuansheng Pan[a]; David Brown[b]; Gervais Chapuis[a]
[a] Institut de cristallographie, Université de Lausanne, Lausanne, Switzerland [b] Laboratoire des Matériaux Organiques à Propriétés Spécifiques, UMR CNRS, Université de Savoie, Le Bourget du Lac, France

Online publication date: 26 October 2010

To cite this Article Pan, Yuansheng , Brown, David and Chapuis, Gervais(2003) 'Molecular Dynamics Simulation of Hexamine and Suberic Acid', Molecular Simulation, 29: 8, 509 — 518
To link to this Article: DOI: 10.1080/0892702031000150561
URL: http://dx.doi.org/10.1080/0892702031000150561

Molecular Simulation, VOL. 29 (8), August 2003, pp. 509–518

Molecular Dynamics Simulation of Hexamine and Suberic Acid

YUANSHENG PAN[a,*], DAVID BROWN[b] and GERVAIS CHAPUIS[a]

[a]*Institut de cristallographie, Université de Lausanne, BSP Dorigny, 1015 Lausanne, Switzerland;* [b]*Laboratoire des Matériaux Organiques à Propriétés Spécifiques, UMR CNRS 5041, Université de Savoie, 73376 Le Bourget du Lac, France*

(Received July 2001; In final form July 2001)

In order to perform a molecular dynamics (MD) simulation of the incommensurate crystalline structure hexamethylenetetramine suberate ($C_6H_{12}N_4$)(HOOC–$(CH_2)_6$–COOH), we present in a first step the separate simulations of the crystalline structure of each of the two pure components, hexamethylenetetramine (HMT) and suberic acid. The domain decomposition parallel MD program *ddgmq* is used for this purpose. A second-generation consistent force field (CFF91) is employed to describe the interactions between atoms. Starting from experimental crystal structures, both pure components were heated from low to high temperatures. Our MD results show that the HMT system can be well represented by CFF91. In the case of suberic acid the layered structure of the crystal is largely preserved although deviations in the unit cell lengths from the experimental values are ~10%. Rather than attempt a complex re-parametrisation of CFF91 we chose to impose a fixed compensating external pressure tensor to correct for the deficiencies of the chosen force field. After optimising this compensating external pressure tensor at one temperature we find that experimental lattice constants and angles can be well reproduced over a range of temperatures.

Keywords: Crystal structure; Atomic simulation; Pressure tensor; Molecular dynamics; Organic crystal

INTRODUCTION

Incommensurate structures are crystals characterised by long-range order but without the three-dimensional periodicity [1]. In addition to sharp Bragg peaks, their diffraction pattern contains so called satellite reflections, which cannot be indexed with three integers only. Incommensurate crystal structures have been detected in all possible types of materials including organic compounds [2].

They have been extensively studied and characterised by diffraction and spectroscopic methods. The techniques of molecular dynamics (MD) simulations have also been used in some rare cases to simulate incommensurate crystals. Parlinski and Chapuis have simulated simple models of incommensurate structures and their phase transitions between commensurate or incommensurate cases [3,4]. Their model consisted of a very large three-dimensional array of a single point atoms placed on the nodes of a hexagonal lattice. Each atom could only move along a direction parallel to the hexagonal axis. Starting from a potential with harmonic and anharmonic terms, many examples of transitions observed experimentally could be simulated. These studies revealed the precise nucleation processes involved in the transition mechanisms. The influence of temperature and pressure on the phase transition mechanisms could also be studied which allowed the establishment of complete phase diagrams.

The main goal of the present study is to use MD techniques with a second generation consistent force field in order to simulate an organic incommensurately modulated crystal structure. We propose in particular to simulate the crystalline structure of hexamethylenetetramine (hexamine) suberate and other members of the family [5,6]. At room temperature, this incommensurate compound forms a layer structure with alternating sheets of hexamine and suberic acid. For the purpose of our simulation, we shall proceed in two steps. We propose in a first step to simulate separately

*Corresponding author.

ISSN 0892-7022 print/ISSN 1029-0435 online © 2003 Taylor & Francis Ltd
DOI: 10.1080/0892702031000150561

the crystalline structure of each component. A successful simulation of hexamine and suberic acid, for which both crystalline structures are well described, is a necessary step before the subsequent simulation of the adduct which forms the incommensurate crystal structure. In this article we present an MD simulation of hexamine and suberic acid.

METHOD AND MODEL

Molecular dynamics simulation is a technique to estimate the equilibrium and transport properties of a classical many-body system [7–9]. The time evolution of a set of interacting atoms is obtained by integrating their equations of motion. The parallel MD program *ddgmq* used in this project was principally designed for the simulation of dense materials in three dimensions (3D) with periodic boundary conditions [10]. The shape and size of the primary MD box is defined by a 3 × 3 matrix **H** made up from the three basis (column) vectors {**a**,**b**,**c**} which allows for non-orthogonal cells. All atoms are subject to a rudimentary force field possibly in the presence of a number of rigid constraints. The atoms can be linked together in an arbitrary way to form molecules of various complexities. The MD system can be simulated either at constant-volume constant-temperature (NVT) conditions [12] or alternatively a required pressure tensor can be applied to give NPT dynamics [13]. In the latter case differences between the internally measured pressure tensor and the externally required pressure tensor may lead to changes in both the box size and shape.

In *ddgmq*, molecules are modelled as a number of atoms connected by a network of bonds. All atoms interact with their "non-bonded" neighbours through a pair potential. The non-bonded pair potentials are the Lennard–Jones (LJ) 9–6 potential

$$\phi_{\mathrm{LJ}}(|r_{ij}|) = A_{ij}|r_{ij}|^{-9} - B_{ij}|r_{ij}|^{-6}$$

and the Coulombic potential

$$\Phi_{\mathrm{C}}(|r_{ij}|) = \frac{q_i q_j}{(4\pi\varepsilon_0|r_{ij}|)}$$

Atom pairs forming a chemical bond can be kept apart at a fixed distance by a rigid constraint

$$|r_{ij}|^2 - b_0^2 = 0$$

or alternatively, quite close to it by a harmonic spring potential

$$\Phi_{\mathrm{b}}(|r_{ij}|) = \frac{1}{2}k_{\mathrm{b}}(|r_{ij} - b_0|)^2.$$

The bond angles are maintained close to their equilibrium values. The bending potential has the following expression:

$$\Phi(\theta) = \frac{1}{2}k_\theta(\cos\theta - \cos\theta_0)^2$$

The bond angle, is defined by the positions of three contiguous atoms, i.e. $\{i, j, k\}$ with i bonded to j, j bonded to k and $i \neq k$),

$$\cos\theta = \frac{(r_{ij}\cdot r_{kj})}{(|r_{ij}||r_{kj}|)}$$

Similarly, given four contiguous atoms in a molecule, torsion potentials are used to represent restricted rotation around the dihedral angles:

$$\Phi_{\mathrm{Tor}}(\tau) = \sum_{m=0}^{6} C_m \cos^m \tau$$

where

$$\cos\tau = -\frac{(r_{ij}\times r_{jk})\cdot(r_{jk}\times r_{kl})}{|r_{ij}\times r_{jk}||r_{jk}\times r_{kl}|}.$$

The motion of central trivalent atoms in planar groups is restricted using out-of-plane potentials of the form

$$\phi_{\mathrm{oop}}(s) = \frac{1}{2}k_{\mathrm{oop}}s^2$$

with

$$s = r_{ji}\cdot\frac{(r_{jk}\times r_{jl})}{|r_{jk}\times r_{jl}|}$$

All the high frequency modes associated with hydrogen atoms in CH_3 and CH_2 groups can be removed using special constraints [24].

All parameters are taken from the consistent force field (CFF91), a second-generation force field [11,14]. In CFF91, a large number of force field parameters are accurately determined by fitting the energy expression to quantum observables (based on quantum mechanics calculations and molecular simulations). Non-bonded parameters are computed by fitting to experimental crystal lattice constants and sublimation energies [15]. The applied parameters are especially adapted for acetyls, acids, alcohols, alkanes, alkenes, amides, amines, aromatics, ethers, and esters [11,14]. This force field has been used to successfully predict lattice parameters, rms atomic co-ordinates and sublimation energies for crystals.

The partial charges assigned automatically by the selected force field (CFF) are identical for the same type of atom independent of their neighbouring atoms. This is not accurate enough for our simulation. In order to improve these parameters,

we used the charge equilibration approach within the Cerius2 package [27,28] that gives more appropriate values for the molecular geometry and the atomic electronegativities. This approach allows the charges to respond to changes in the environment. The resulting values are in good agreement with the experimental dipole moments and with the result from the electrostatic potentials of accurate *ab initio* calculations [28].

In our simulation, the time step is one femtosecond. The Ewald method is employed to handle the Coulombic potential for which a simple truncation is not justified due to the slow convergence of the sum of terms decaying as $1/r$. Three parameters, the Ewald separation parameter α, the real space potential truncation range R_{max} and the upper bound of the range of k-vectors in the reciprocal space part for the Ewald summation K_{max} are used to optimise the convergence of the Coulombic energy [16]. Using $\alpha = 0.4\text{Å}^{-1}$, $R_{max} = 9\,\text{Å}$ and $K_{max} = 8$ in the simulation of the HMT system, the difference between direct and implied reciprocal space summation part of the pressure [17] is relatively small, in MD terms, at about 10 bar. In the suberic acid system, the Ewald parameters are $\alpha = 0.3\,\text{Å}^{-1}$, $R_{max} = 9\,\text{Å}$ and $K_{max} = 9$ for a similar level of convergence. There are $3 \times 3 \times 3$ unit cells with 54 molecules (each with 22 atoms) in the HMT system. The suberic acid system has $8 \times 4 \times 8$ unit cells with 512 molecules (each with 26 atoms). NPT calculations were performed for heating or cooling the system. The validity of the force field parameters can be checked by comparing the simulation results with the experimental results obtained by X-ray diffraction.

The molecular structure of hexamethylenetetramine HMT ($C_6H_{12}N_4$) is shown in Fig. 1a. The cubic space group is $I\bar{4}3m$. The highly symmetric crystal structures were determined at seven different temperatures from neutron and X-ray diffraction data by Kampermann and Terpstra [18,19]. The experimental structure at 15 K was taken as the starting model of our MD simulation.

Suberic acid ($COOH(CH_2)_6COOH$) is a fatty acid whose crystal structures were experimentally obtained at six different temperatures [20,21]. The starting structure for the MD simulation is shown in Fig. 1b which represents the experimental model at 18.4 K. The space group is $P2_1/c$ with two molecules per unit cell. This system was subsequently heated to higher temperatures. The charges obtained initially from CFF and those resulting from the subsequent

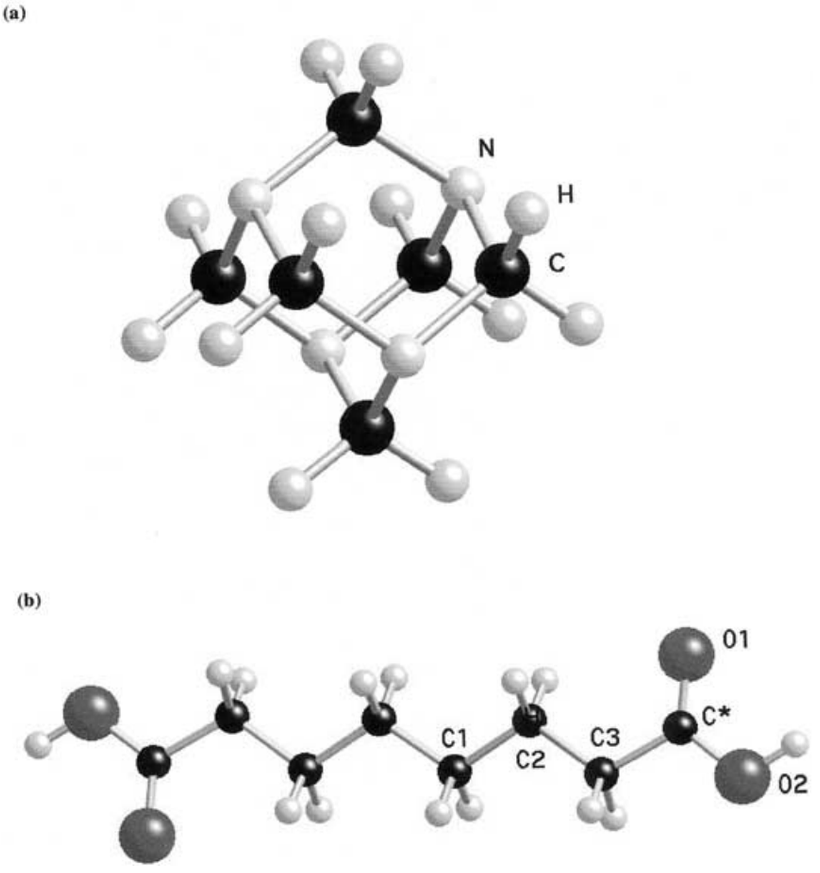

FIGURE 1 Molecular structures: (a) HMT, (b) suberic acid.

TABLE I Charges (*e*) assigned by CFF and by the equilibration procedure at 18.4 and 298 K to the suberic acid molecule. See Fig. 1 for the atom identification

		Equilibration	
Atom	*CFF*	18.4 K	298 K
C1	−0.1060	−0.3020	−0.4504
C2	−0.1060	−0.2971	−0.3991
C3	−0.1060	−0.1216	−0.1650
C*	0.3994	0.5741	0.5951
O1	−0.3964	−0.6182	−0.6168
O2	−0.4271	−0.6915	−0.6353
H(O2)	0.4241	0.4105	0.3962
H1(C1)	0.0530	0.1609	0.2296
H2(C1)	0.0530	0.2038	0.2458
H1(C2)	0.0530	0.1449	0.2019
H2(C2)	0.0530	0.2008	0.2442
H1(C3)	0.0530	0.1178	0.1476
H2(C3)	0.0530	0.2166	0.2052

charge equilibration procedure are presented in Table I.

SIMULATION RESULTS

HMT

In this molecule, the atoms involved are C, N and H with charges 0.042, −0.390 and 0.109*e* obtained from the equilibration approach. The initial charges from CFF are 0.059, −0.248 and 0.053*e*, respectively. Each atom appears only in one single type. Starting with the experimental structure at 15 K, the HMT system was heated up to 600 K. The simulations were performed using NPT with a fixed heating rate of $0.5\,\mathrm{K\,ps^{-1}}$.

After reaching the required temperature, the crystal structure obtained from the simulation results is used to generate a powder diffraction pattern. The software DISCUS [22] was used to generate the powder diffractogram. Diffraction patterns for structures simulated at 50, 80, 120, 160 and 200 K are presented in Fig. 2. The corresponding pattern at 15 K based on diffraction results is also shown. The direct comparison shows already the close similarities between the experimental and simulated patterns.

The average lattice constants and angles of the HMT system can also be obtained from the simulation results. The simulation and experimental data are presented in Table II. It appears that the simulated lattice constants are greater than the experimental data. The difference between them increases with temperature from about 0.4 to 1%. The three angles α, β and γ are almost equal to 90°, which indicate that the system maintains its high symmetry. The average C–N bond distance was also measured for some temperatures. They agree well with the experimental results.

The phase transition of the HMT system was also studied in the temperature range from 15 to 600 K by MD simulation. Figure 3 gives the variations of intermolecular energy, density and mean square displacement with temperature. The three curves exhibit significant changes at ~400 and ~500 K. The mean square displacement converges to a finite value before ~400 K. In other words, the HMT system is solid below this temperature. Above this temperature, the mean square displacement grows steadily with time, which implies that the system is liquid between ~400 and ~500 K. The system becomes gaseous at temperatures above ~500 K. Experimental melting and boiling points could not be found for the HMT system. The only experimental result concerns the sublimation temperature [23] at 553 K. The transition at ~500 K in the model system probably corresponds closest to the sublimation temperature owing to the important change in the intermolecular energy at this point. The enthalpy of sublimation can be obtained from the intermolecular

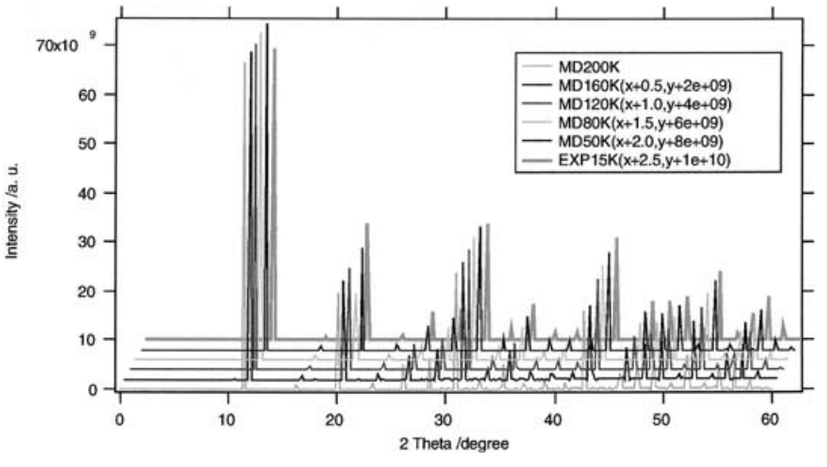

FIGURE 2 Simulated powder diffraction patterns of the HMT system (neutron with 1 Å wavelength). The "EXP15" pattern results from the crystal structure obtained from single crystal at 15 K. The other patterns are based on molecular dynamics simulation structures.

TABLE II A comparison of experimental and simulated lattice constants (in Angstroms and degrees) for HMT. The error bars in the MD results for average unit cell lengths and angles are determined from the fluctuations and correlation in the data to be ~0.02 Å and ~0.01°, respectively

		MD simulation results					
Temperature (K)	*Exp. lattice constants*	***a***	***b***	***c***	α	β	γ
15	6.9274	6.93	6.93	6.93	90.00	89.99	90.00
50	6.9337	6.95	6.95	6.95	89.98	89.99	90.01
80	6.9424	6.96	6.96	6.96	89.96	90.01	90.01
120	6.9551	6.98	6.98	6.98	90.05	90.00	89.98
160	6.9693	7.00	7.00	7.00	89.99	90.00	90.01
200	6.9835	7.02	7.02	7.02	89.98	90.02	90.03
298	7.0280	7.10	7.10	7.10	89.92	90.04	90.09

energy. It is about 78.2 kJ mol^{-1} per molecule at 316 K. From experimental results [25], the corresponding enthalpy of sublimation is 78.8 kJ mol^{-1} per molecule at the same temperature.

Suberic Acid

Starting the MD simulations of the suberic acid system with the experimental structure at 18.4 K and the charges obtained from the charge equilibration approach at this temperature, the system was heated to 700 K at the rate of 2 K ps^{-1}. After reaching 18.4, 50, 75, 100, 123, 298 K, the crystal structures of the system were extracted from the simulation results. They were used to generate their corresponding powder diffraction patterns. Figure 4 shows the simulated patterns and the experimental diffractogram at 18.4 K. The comparison shows that differences of 0.3 and 0.1° exist between the first and second strongest peaks, corresponding to differences in the interlayer spacing of $\Delta d = -0.08$ and -0.06 Å, respectively. However, we can clearly identify the crystalline phases of suberic acid.

The average lattice constants and angles of the simulated systems were evaluated for all of the temperatures reported above and they are compared with experimental results [21,22] in Table III. The differences between them are about -11% for ***a***, less than 2% for ***b***, and from 5 to 10% for ***c*** and from 0.5 to 2% for the angle β. The phase transitions of suberic acid were investigated from the simulation results. Figure 5 shows the percentage of C–C–C*–O(H) torsion angles in the *trans* state, intermolecular energy and mean square displacement as a function of temperature. In this system, molecules are connected by hydrogen bonds when in the crystal state. So the percentage of C–C–C*–O(H) torsion angles that are *trans* is also a good indication of melting and boiling. According to the three curves, the system is solid for temperatures below ~580 K, liquid between ~580 and ~740 K and gaseous above ~740 K. Experimental results give the melting point at 417 K and the boiling point at 492.5 K [23]. From Fig. 5, it can be seen that the sublimation energy at ~298 K is ~201 kJ mol^{-1} for the model system. The corresponding experimental value is 148 kJ mol^{-1} at 298 K [26]. The larger sublimation energy probably

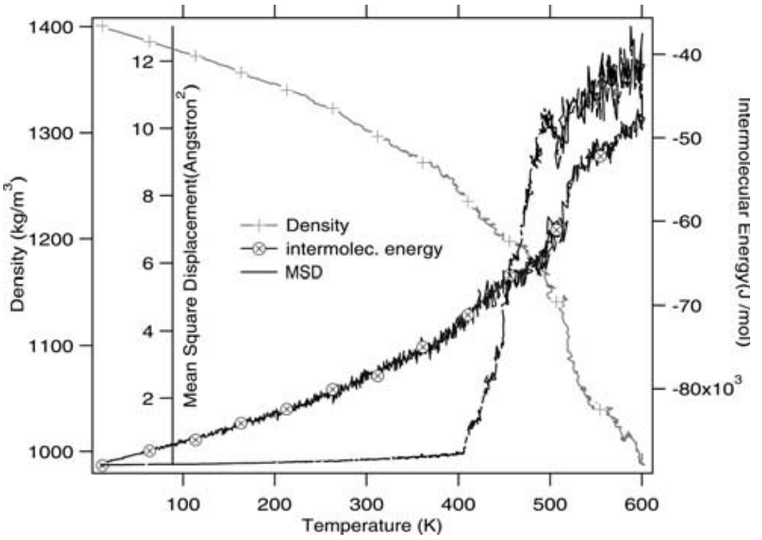

FIGURE 3 Phases transitions of the HMT system.

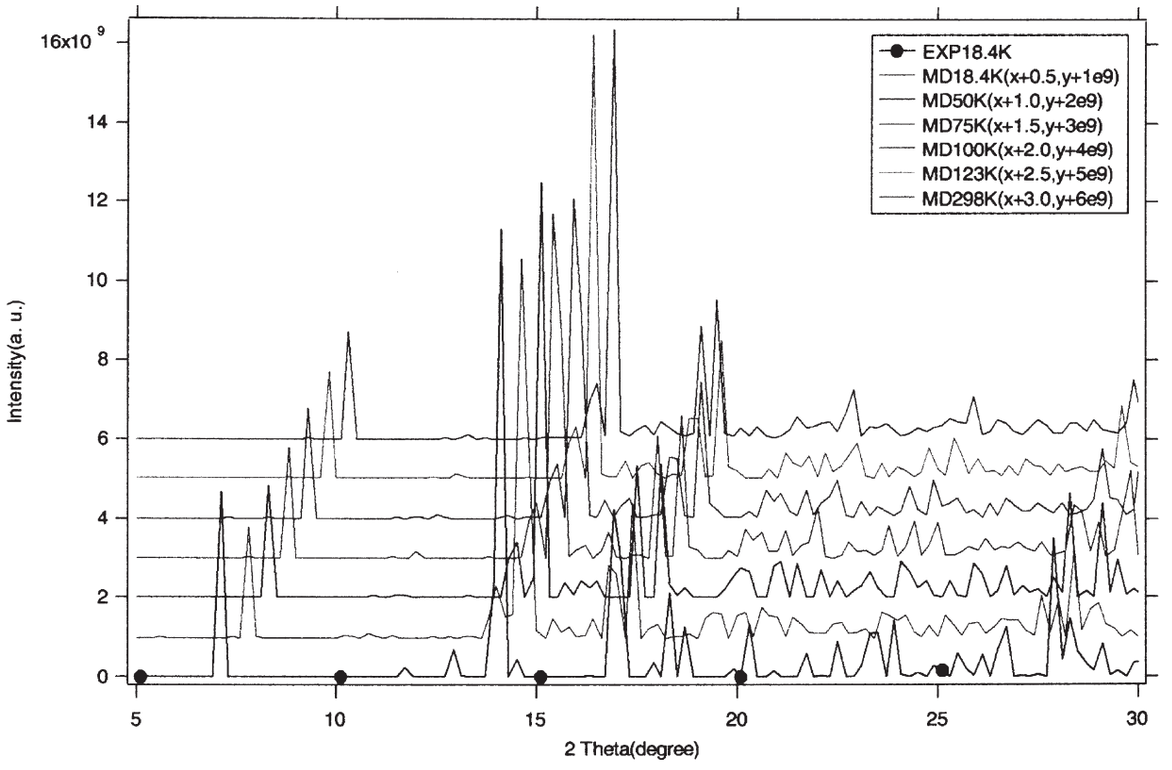

FIGURE 4 Simulated powder diffraction patterns of the suberic acid system (neutron with 1 Å wavelength). The "EXP18.4 K" pattern is using experimental data measured at 18.4 K. All other patterns are based on structures from molecular dynamics simulations.

accounts for the shift to higher temperatures of the simulated melting and boiling points.

Suberic Acid System Using a Compensating Pressure Tensor

In the suberic acid simulations described in the previous section, the starting structure was taken directly from the experiment results at 18.4 K. The shape and size of the crystal moved rather much away from this during the simulation even at this low temperature. We attribute this to deficiencies in the force field, particularly the interactions between molecules. The previous results show that such differences persist over the entire temperature regime where comparisons can be made with experiment.

To reproduce better the experimental structure some re-parametrisation of the non-bonded potential is clearly required. This is not that straightforward, however, and is not really one of the aims of this work. Rather we ultimately want to use the same force field for adduct systems containing HMT and a range of dicarboxylicacids. As performing a global re-optimisation of CFF91 for dicarboxylicacids is not our intended goal we have instead chosen a different, more pragmatic, approach to the problem. A compensating external pressure tensor is instead applied to compensate for the deficiencies in the interactions between molecules. This compensating

TABLE III A comparison of experimental and simulated lattice constants (in Angstroms and degrees) for suberic acid. The error bars in the MD results for average unit cell lengths and angles are determined from the fluctuations and correlation in the data to be ~0.005 Å and ~0.05°, respectively

Temperature (K)		***a***	***b***	***c***	α	β	γ
18.4 K	Exp.	8.710	5.089	9.815	90.00	95.07	90.00
	MD	7.730	5.045	11.120	88.15	98.05	88.25
50 K	Exp.	8.723	5.0861	9.831	90.00	95.25	90.00
	MD	7.775	5.100	10.983	89.98	97.21	90.01
75 K	Exp.	8.742	5.084	9.850	90.00	95.43	90.00
	MD	7.785	5.165	10.875	90.20	96.50	89.65
123 K.	Exp.	8.784	5.072	9.889	90.00	95.95	90.00
	MD	7.805	5.140	10.980	90.20	97.25	89.85
298 K	Exp.	8.98	5.06	10.12	90.00	97.50	90.00
	MD	7.900	5.145	11.225	90.25	99.10	90.40

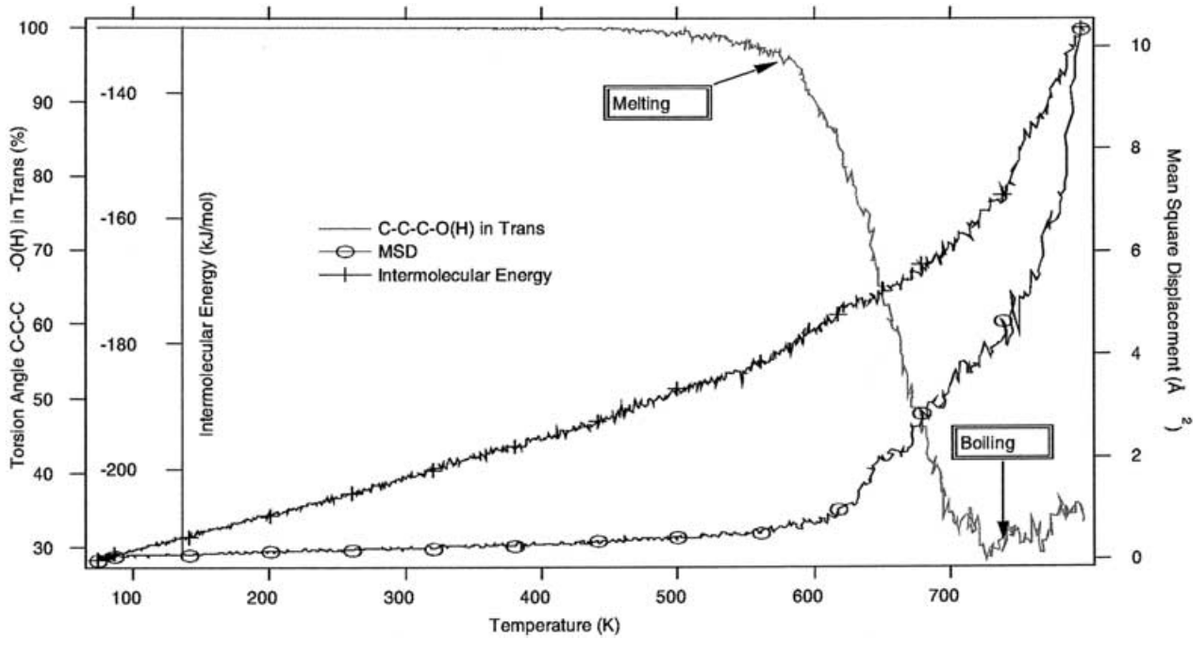

FIGURE 5 Phases transition of the suberic acid system.

pressure tensor field is first determined by using NVT dynamics at the experimentally determined box size and shape at a chosen temperature. The average pressure tensor that results from this NVT simulation then becomes the compensating external pressure tensor for all temperatures.

In this new simulation, a $16 \times 8 \times 8$ unit cell suberic acid system was set up in the experimental structure at 298 K. In this case the charges used were those resulting from charge equilibration at 298 K. These charges are also listed in Table I. We first let the system equilibrate under NVT conditions and then the average pressure tensor was determined; the values found are given in Table IV.

Using the compensating external pressure tensor given in Table IV, the system was first cooled to 45 K and then heated to 684 K. Lattice constants from the simulation are plotted in Fig. 6. For comparison, experimental results were also plotted in Fig. 6. A detailed comparison of lattice constants between simulation and experiment are presented in Table V. From these results, we find the simulation reproduces better the experimental lattice constants. So the applied pressure tensor field can compensate for the deficiencies in the force field.

Phase transitions were also investigated in this system. Figure 7 gives changes in the percentage of C–C–C*–O(H) torsion angles in the *trans* state, mean square displacement and intermolecular energy from 298 to 684 K. The melting and boiling temperature were determined at 560 and 630 K. The sublimation energy at 298 K is 179 kJ mol^{-1} which is closer to the experimental value owing to the application of a compensating pressure tensor.

DISCUSSION AND CONCLUSION

Using the CFF91 force field in the parallel MD program *ddgmq*, both hexamine and suberic acid systems have been simulated. The crystalline starting structures for the MD simulations were taken from experimental X-ray diffraction results. By heating the systems from low to high temperatures under NPT conditions, where both the box size and shape are free to adjust to an external pressure tensor, it has been established that both HMT and suberic acid have a wide range of crystalline stability. The pseudo-powder diffractograms generated from the simulations at various temperatures show a reasonable similarity with experiment indicating no large-scale differences in crystal structure occurs; as is confirmed by a visual inspection. In the case of HMT the cubic symmetry is very well reproduced and a maximum error of $\sim$1% is found for the unit cell length over the range from 15 to 298 K of the experimental data.

TABLE IV Compensating pressure tensor for suberic acid system (in bar)

	x	y	z
x	−1790	0	1070
y	0	−400	0
z	1070	0	3880

TABLE V A comparison of experimental and simulated lattice constants (in Angstroms and degrees) for suberic acid subject to the compensating pressure tensor given in Table III. The error bars in the MD results for average unit cell lengths and angles are determined from the fluctuations and correlation in the data to be ~ 0.005 Å and $\sim 0.05°$, respectively

Temperature (K)		***a***	***b***	***c***	α	β	γ
50 K	Exp.	8.723	5.0861	9.831	90.00	95.25	90.00
	MD	8.675	4.945	10.135	90.00	96.05	90.00
75 K	Exp.	8.742	5.0841	9.850	90.00	95.43	90.00
	MD	8.685	4.980	10.110	90.00	95.95	90.00
100 K	Exp.	8.761	5.0792	9.871	90.00	95.69	90.00
	MD	8.700	5.005	10.105	90.00	96.00	90.00
123 K	Exp.	8.784	5.072	9.889	90.00	95.95	90.00
	MD	8.715	5.015	10.110	90.00	96.10	90.00
298 K	Exp.	8.98	5.06	10.12	90.00	97.50	90.00
	MD	8.948	5.065	10.153	90.01	97.45	90.02

In the case of suberic acid the monoclinic symmetry is well maintained with α and γ approximately 90° except at the very lowest temperatures studied. The β angle is systematically higher, however, at all temperatures but, the 18.4 K data apart, no more than 2°. This increase in the tilt angle is accompanied by a contraction along the **a** axis of about 10% and a compensating extension of the ***c*** axis by 10%, the ***b*** length remaining quite close to the experimental value. This we attribute to a deficiency in the non-bonded part of the CFF91 potential. The increased tilt angle and the reduction of the ***a*** length implies a closer packing of the chains in a direction perpendicular to their axes compared to experiment. The concomitant increase in the **c** length leads us to suspect that the balance of the interlayer forces perpendicular and parallel to the chain axes is not quite correct. As the interlayer forces parallel to the chain axes are significantly influenced by the hydrogen bonds between the carboxylic acid groups this imbalance may boil down to a question of the relative strengths of the van der Waals versus Coulombic forces.

In the simulation of both compounds, the charges resulting from the equilibration approach have been used. These charges are based only on the geometry and experimental atomic properties and are more accurate than the CFF charges.

Even though CFF91 is a best overall fit to experimental results for a range of carboxylic acids and amides [26], the accuracy that it achieves in the description of intermolecular interactions is still far from the resolution that can be obtained in crystallography. By introducing an external compensating pressure tensor, we can at least largely correct for the deficiency in the potential and have a closer correspondence between the simulated and experimental unit cell geometry. This we believe is necessary when trying to simulate incommensurate structures where subtle differences in packing can have a large influence. Therefore, the compensating pressure is necessary in order to reproduce

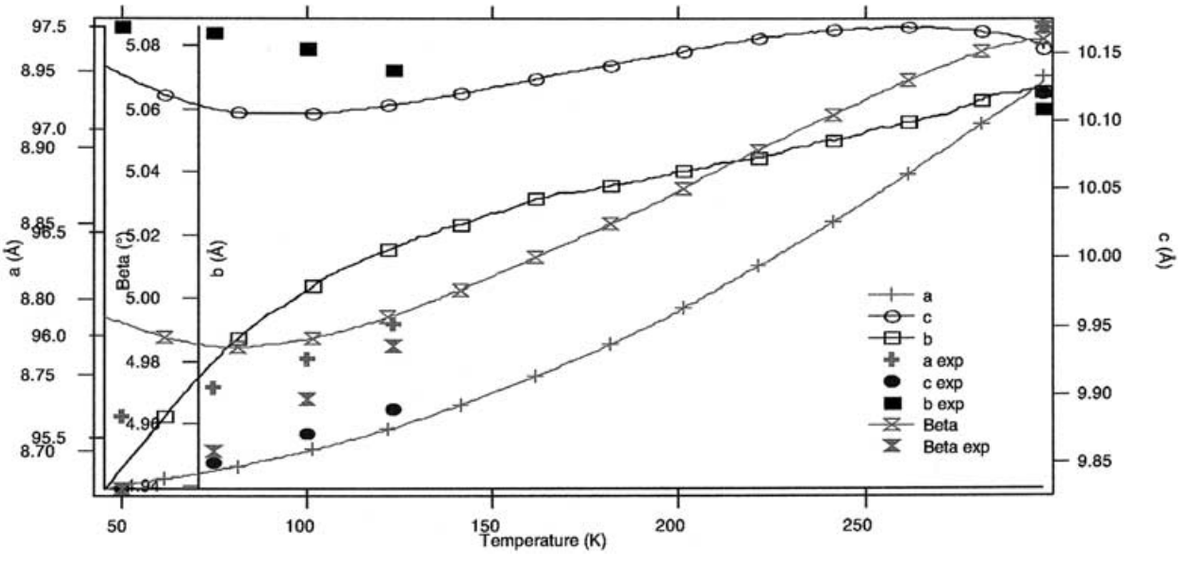

FIGURE 6 Lattice constants and angle of suberic acid system with compensating pressure tensors field.

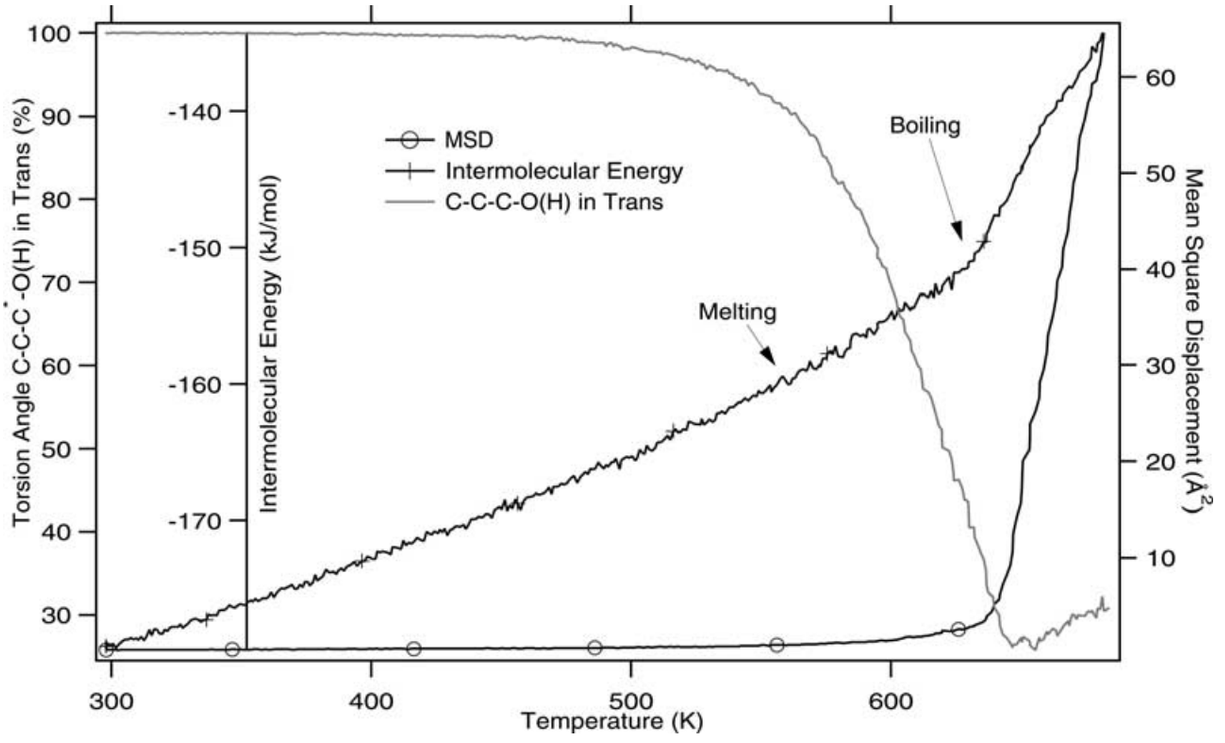

FIGURE 7 Phases transition of suberic acid system with compensating pressure tensor.

the sequence of phases and the other properties depending on the structure.

The comparison carried out using the suberic acid system, for which experimental data stretches over a wide regime, confirms that the compensating pressure tensor evaluated at one particular temperature is transferable to other temperatures. This is an important point to establish as it reinforces the suspicion that the intermolecular forces are largely at fault. It is also useful as in general the unit cell geometry may only be known at one temperature and this gives us confidence in applying it in other regimes.

The program DISCUS [22] is very effective in analysing the MD results and generating the pseudo-diffraction patterns. It will be particularly useful in the next stage of the project where we will use it to detect signs of incommensurate behaviour. The structural origin of the incommensurability can then be studied by closely examining the details of the packing of the molecules.

MD simulation results provide much detail information about crystal structures. At present, the simulations are limited by the CPU to relatively small system sizes and time interval. For the simulation of incommensurate systems, which are non-periodic in some special directions, the MD simulation box should be large enough to encompass the incommensurability length scale. A balance between system size and running time has thus to be achieved. We are currently applying MD techniques to simulate incommensurate crystal structures. This work will be presented in a future publication [29].

Acknowledgements

This work is supported by the Swiss National Science Foundation which is gratefully acknowledged (Grant No. 20-56870.99). The authors are indebted to the generous support of the Swiss Centre for Scientific Computing (CSCS) and the Computing Centre of the Federal school of Technology in Lausanne (EPFL) for providing resources on the SX-4/SX-5 and Swiss T1 computers, respectively.

References

[1] Janssen, T. and Janner, A. (1987) "Incommensurability in crystals", *Adv. Phys.* **36**, 519–624.
[2] Yamamoto, A. (1996) "Crystallography of quasiperiodic crystals", *Acta Crystallogr.* **A52**, 509–560.
[3] Parlinski, K. and Chapuis, G. (1993) "Mechanisms of phase transitions in a hexagonal model with 1*q* and 3*q* incommensurate phase", *Phys. Rev.* **B47**, 13983–13991.
[4] Parlinski, K. and Chapuis, G. (1994) "Phase-transition mechanisms between hexagonal commensurate and incommensurate structures", *Phys. Rev.* **B49**, 11643–11651.
[5] Gaillard, V.B., Paciorek, W., Schenk, K. and Chapuis, G. (1996) "Hexamethylenetetramine suberate, a strongly anharmonic modulated structure", *Acta Cryst.* **B52**, 1036–1047.

[6] Gaillard, V.B., Chapuis, G., Dusekand, M. and Petricek, V. (1998) "Hexamethylenetetramine sebacate, an incommensurate structure with large nonsinusoidal modulations: comparison of two refinement strategies", *Acta Cryst.* **A54**, 31–43.
[7] Allen, M.P. and Tildesley, D.J. (1987) *Computer Simulation of Liquids* (Clarendon Press, Oxford).
[8] Haile, J.M. (1992) *Molecular Dynamics Simulation: Elementary Methods* (Wiley, New York).
[9] Frenkel, D. and Smit, B. (1996) *Understanding Molecular Simulation: From Algorithms To Applications* (Academic Press, San Diego).
[10] Brown, D., Minoux, H. and Maigret, B. (1997) "A domain decomposition parallel processing algorithm for molecular dynamics simulations of arbitrary connectivity", *Comp. Phys. Commun.* **103**, 170–186. See also "The gmq User Manual Version 3", available at http://www.univ-savoie.fr/labos/lmpc/db.html; D. Brown and B. Maigret, "Large Scale Molecular Dynamics Simulations using the Domain Decomposition Approach", Speedup Proceedings of the 24th SPEEDUP Workshop, Berne 24–25th Sept. 1998, Vol. 12(2), pages 33–41 (Oct. 1999).
[11] Maple, J.R., Hwang, M.-J., Stockfisch, T.P., Dinur, U., Waldman, M., Ewig, C.S. and Hagler, A.T. (1994) "Derivation of class II force fields. 1. Methodology and quantum force field for the alkyl functional group and alkane molecules", *J. Comput. Chem.* **15**, 162–182.
[12] Berendsen, H.J.C., Postma, J.P.M., van Gunsteren, W.F., DiNola, A. and Haak, J.R. (1984) "Molecular dynamics with coupling to an external bath", *J. Chem. Phys.* **81**, 3684–3690.
[13] Brown, D. and Clarke, J.H.R. (1991) "A loose coupling constant pressure molecular dynamics algorithm for use in the modelling of polymer materials", *Comput. Phys. Commun.* **62**, 360–369.
[14] Hwang, M.-J., Stockfisch, T.P. and Hagler, A.T. (1994) "Derivation of class II force fields. 2. Derivation and characterization of a class II force field, CFF93, for the alkyl functional group and alkane molecules", *J. Am. Chem. Soc.* **116**, 2515–2525.
[15] Hagler, A.T., Dauber, P. and Lifson, S. (1979) "Consistent force field studies of intermolecular forces in hydrogen-bonded crystals. 1. Carboxylic acids, amides, and the C=O...H-hydrogen bonds. 2. A benchmark for the objective comparison of alternative force field", *J. Am. Chem. Soc.* **101**, 5122–5130.
[16] Smith, W. (1986) "Optimising the Ewald sum. Information quarterly for computer simulation of condensed phases", *The CCP5 Newslett.* **21**, 37.
[17] Brown, D. and Neyertz, S. (1995) "A general pressure tensor calculation for molecular dynamics simulations", *Mol. Phys.* **84**, 577–595.
[18] Kampermann, S.P., Sabine, T.M., Craven, B.M. and Mcmullan, R.K. (1995) "Hexamethylenetetramine: extinction and thermal vibrations from neutron diffraction at six temperatures", *Acta Cryst.* **A51**, 489–497.
[19] Terpstra, M., Craven, B.M. and Stewart, R.F. (1993) "Hexamethylenetetramine at 298 K: new refinements", *Acta Cryst.* **A49**, 685–692.
[20] Gao, Q., Weber, H.P., Craven, B.M. and Mcmullan, R.K. (1994) "Structure of suberic acid at 18.4, 75 and 123 K from neutron diffraction data", *Acta Cryst.* **B50**, 695–703.
[21] Housty, P.J. and Hospital, M. (1965) "Localisation des atomes d'hydrogéne dans l'acide subérique $COOH(CH_2)_6COOH$", *Acta Cryst.* **18**, 753.
[22] Proffen, Th. and Neder, R.B. (1997) "DISCUS: a program for diffuse scattering and defect structure simulations", *J. Appl. Cryst.* **30**, 171–175.
[23] (1988) "CRC Handbook of Chemistry and Physics", (CRC Press.
[24] Hammonds, K.D. and Ryckaert, J.-P. (1991) "On the convergence of the SHAKE algorithm", *Comput. Phys. Commun.* **62**, 336–351.
[25] De Wit, H.G.M., VanMiltenburg, J.C. and De Kruif, C.G. (1983) "Thermodynamic properties of molecular organic crystals containing nitrogen, oxygen, and sulphur. 1. Vapour pressures and enthalpies of sublimation", *J. Chem. Thermodyn.* **15**, 651–663.
[26] Hagler, A.T., Lifson, S. and Dauber, P. (1979) "Consistent force field studies of intermolecular forces in hydrogen-bonded crystals. 1. Carboxylic acids, amides, and the C=O...H-hydrogen bonds", *J. Am. Chem. Soc.* **101**, 5122–5130.
[27] Cerius2, Molecular Simulations, San Diego, 1997.
[28] Rappé, A.K. and Goddard, W.A. (1991) "Charge equilibration for molecular dynamics simulation", *J. Phys. Chem.* **95**, 3358.
[29] Pan, Y., Brown, D. and Chapuis, G. (2002) "Mechanism of the incommensurate phase in hexamethylene-tetramine suberate: A molecular dynamics study", *Phys. Rev. B*, **65**(18), 184205/1–8.